International Journal of Applied Mathematics
Volume 38 No. 10s, 2025
ISSN: 1311-1728 (printed version); ISSN: 1314-8060 (on-line version)

IMPROVEMENT OF IMAGE RESOLUTION FOR AN OPTICAL SYSTEM WITH A HANNING AMPLITUDE FILTER

Nada Qasim 1 **, Abdul Haleem A. Raheem** 2**, Duha A.Kadhim 3, Ghada S. Karam 4**

1,2,3 Department of Physics, College of Science, Mustansiriyah University, Baghdad, Iraq

4Department of Physics, College of Education, Mustansiriyah University, Baghdad, Iraq

a) Nada.q.94@uomustansiriyah.edu.iq
b) Abd.alhaleim.A.R@oumstansiriyah.edu.iq
c) duha.abdual@uomustansiriyah.edu.iq

Abstract:

The key information of images is typically embedded in their configuration, specifications, and surroundings. These components require unique processing techniques to improve image resolution adequately. In this paper, we develop a formula capable of significantly improving image sharpness and clarity using the point spread function (PSF) equation for a rectangular aperture and a triangular aperture optical system using Mathcad. The Hanning amplitude filter (β=0, 0.25, 0.50, 0.75, 1) is applied as the image enhancement technique. The research addresses an optical system constrained by diffraction limits (an ideal system). The two apertures of the optical system are compared, and the full width at half maximum of half of each curve, a measure of the spectral linewidth, is measured. The results are presented graphically.

Keywords: imaging systems**,** optical system, point spread function, Hanning amplitude filter, pupil function.

Introduction:

The objective of lens makers is to assess the effectiveness of that lens, which reflects the precision of that optical design, by evaluating picture quality. A multitude of elements significantly influence the assessment of picture quality in the imaging system [1]. One factor is wave front aberration, which includes issues such as coma, spherical aberration, field curvature, and astigmatism, intrinsic to optical systems; however, alignment or manufacturing errors, along with ergonomic issues, can introduce more aberrations. The defocus effect results in the longitudinal displacement of the focal point from the anticipated Gaussian point, propagating the ray from the centre maxima to the lateral lobes. Correction of optical lens flaws and spherical aberration is mostly accomplished through the use of filters [2]. Although the amplitude filter lowers aberrations, the light that the optical system transmits is sacrificed in the process [3]. Since the majority of optical functions may be thought of as being generated from the picture

Received: August 03, 2025

International Journal of Applied Mathematics
Volume 38 No. 10s, 2025
ISSN: 1311-1728 (printed version); ISSN: 1314-8060 (on-line version)

plane (PSF) by a differential or integral connection, the second element is the ascertainment of the intensity distribution in one PSF [4].

The intensity of distribution at a point in that picture, a plane of a point object, such as a sharp or straight edge, is described by the PSF. The kind and degree of aberration in the lens, as well as the diffraction produced by the aperture, determine the intensity distribution. As a result, it frequently combines several optical phenomena, such as veiling glare, defocus, aberration, and diffraction. The most popular metric for estimating the distribution of energy along the optical axis and assessing the quality of PSF close to the focal plane was the Strehl ratio [5]. One method that is comparable to the characteristics of an imaging optical system is apodization. In instrumental optics, several apodization filters have been suggested for a variety of uses]6[. Visual optical systems either have aberrations or are constrained by diffraction (ideal system). In optical processing, using a flawless system is crucial for assessing any system's effectiveness. Particularly when taking into account both internal (like vibration or optical system movement) and exterior (like the actual presence of clouds, fog, or dust) affecting variables [7]. The mathematical techniques that are now accessible provide a clear picture of the image quality when both internal and external affecting factors are present.

In our previous paper[8], we studied the optical properties of a circular aperture optical system for a diffraction-limited system and applied a parabolic filter. Initial results indicated that the numerical results appear to be an improvement over the standard method. In this paper, we studied the properties of an ideal diffraction-limited optical system and applied a Hanning amplitude filter. The central maximum width was calculated to achieve good resolution for rectangular and triangular aperture optical systems. A comparison between these two apertures was made, and the results were presented.

An essential image evaluation criterion for discussing the intensity distribution in the imaging plane is HWHM, or half-width at half-maximum, which is estimated 50% out of the primary peak's peak intensity is the estimated distance at the diffraction canter [9].

Related work:

A number of researchers have examined diverse techniques to alter the aperture in order to enhance image quality when the aperture's size and shape impact an image's structure. Ali H. Al-Hamadani et al[10] assessed the resolving power of an optical system in relation to pupil shapes. Under the effect of coma aberration, these systems are apodized using the amplitude filter of Hanning. Graphical representations of the analytically calculated results are provided by point spread function graphs under various aberration of coma concerns, as well as amplitude apodization levels. According to this study, a system with a half diagonal square aperture (1) possesses an elevated Strehl ratio. Additionally, the apodized Hanning filter has the least effect

International Journal of Applied Mathematics
Volume 38 No. 10s, 2025
ISSN: 1311-1728 (printed version); ISSN: 1314-8060 (on-line version)

on systems with a half diagonal square aperture ($\sqrt{\frac{\pi}{2}}$). Devi et al[11] formulated an expression for the point spread function of an apodized optical system, a Gaussian filter. The calculated outcome is completed for multiple scenarios of apodized parameters. Ban et al [12] This study encompasses the formula of the point spread function (PSF), formulated for a series of concealed circular synthetic apertures. It examines the impact of varying obscuration ratios (ε = 0, 0.25, 0.5, 0.75). Mathcad applications were employed to replicate the PSF equation derived from this analysis. The outcome is an enhancement in the secondary peaks' intensity and superior power for resolution in comparison to the resolving power of a concealed singular circular aperture. Narsaiah et al [13] investigated the impact of the filter to determine the optimal apodization value for an annular aperture, aiming to achieve the minimal radius for the initial dark ring, which subsequently affects the resolution characteristics of optical imaging systems. Campos et al [14] investigated the impact of various amplitude, complex, and phase filters applied to axial and transverse dimensions characteristics pertaining to an optical system, and endeavoured to regulate the amplitude and phase within the LC-SLM to facilitate the implementation of a pupil filter.

Venkanna et al[15] calculated the point spread function of a deviated optical system using apodized Lanczos, Hanning, and amplitude filters for a coherent optical system with rotationally symmetric.

<u>The formula of the point spread function (PSF):</u>

A function, when it comes to point spread, represents a single-point source radiation picture within a system of optics. One may derive this process via this function by taking the complex amplitude of the function when both u and v are in the picture plane and transforming it to use the Fourier transform [16] [17].

$$A(u,v) = \frac{1}{A.S}\iint f(x,y).\,e^{i.2.\pi(u.x+v.y)}\,dxdy \ldots\ldots.(1)$$

This may be stated as where A(u, v) is the amplitude at point (u,v), denoted as (A.S), represents

The area of the exit pupil, whereas f(x, y) is the function that denotes the role of the pupil (1):

$$f(x,y) = \tau(x,y)\cdot e^{ikW(x,y)} \ldots\ldots (2)$$

τ(x, y): "Pupil transparency" describes the authentic distribution of amplitude inside the exit pupil; under homogeneous light, it typically equals one unit.

Received: August 03, 2025

International Journal of Applied Mathematics
Volume 38 No. 10s, 2025
ISSN: 1311-1728 (printed version); ISSN: 1314-8060 (on-line version)

$e^{ikw(x+y)}$: The wave front regarding the function of aberration, w(x,y), represents the aberration coefficient. The point spread function is represented through the intricate amplitude squared in the picture [18]:

$$PSF = |A(u,v)|^2 \ldots\ldots (3)$$

$$PSF = R|\iint f(x,y).e^{i2\pi(ux+vy)}\, dxdy|^2 \ldots\ldots (4)$$

Where R is the normalization constant.

$f(x.y) = (\cos(\pi\beta r^2))^{\frac{1}{2}}$: equation of the Hanning amplitude filter[19].

Let z=2πu and m=2πv; hence, equation (4) transforms into:

$$PSF = |R\iint f(x,y).e^{i(zx+my)}dxdy|^2 \ldots\ldots (5)$$

Due to the symmetry, we shall consider just one axis; so, equation (5) is expressed as follows:

$$PSF = |R\iint f(x,y).e^{i(zx)}dxdy|^2 \ldots\ldots (6)$$

The amalgamation boundary for the point spread function is determined through the aperture pertaining to the optical system; the study employed a horizontal rectangular aperture and a triangular aperture.

The boundaries of a rectangular lens aperture are ascertained using the rectangular pupil aperture within an area normalized by π, the measurement of the length of the horizontal dimension, and the extent of the vertical edge (2). Consequently, equation(6) for a diffraction-limited optical system possessing a rectangular lens aperture will be[20]:

$$PSF = R|\int_{-\pi/4}^{\pi/4}\int_{-1}^{1} f(x,y).\ e^{izx}\, dxdy|^2 \ldots\ldots (7)$$

When the optical system has a triangular aperture, the point diffusion function equation is as in Equation No. 8, and the results were extracted using MathCAD.

$$PSF = R|\int_{-1}^{1}\int_{-\pi/4\,(1-y)}^{\pi/4\,(1-y)} f(x,y).\ e^{izx}\, dxdy|^2 \ldots\ldots (8)$$

The Strehl ratio (SR) was also calculated and is characterized as the proportion of the center intensity of the point spread function (PSF) of the optical system and the regular pupil function of the diffraction-limited system. The Strehl criterion is a suitable measure of the quality of the image formed in lenses[21]:

$$SR^{\circ} = \frac{PSF(H)}{PSF(A)} \ldots\ldots\ldots (9)$$

Where parameters A and H are applied to the Hanning filter, respectively.

Hence [22] [23][24][25], examining the imaging characteristics of optical systems through the understanding of intensity distribution possesses emerged as a crucial approach in the design and evaluation of these systems.

Discussion and results

We calculated the intensity numerically for the amplitude Hanning filter for non-coherent light sources. The filter is placed concerning the rectangular aperture of the polarised optical system, and the intensity is calculated from equation (7) using Mathcad. The results of the PSF intensity values are listed in Table 1. They were plotted in the origin program and shown in the form of curves showing the distribution of the PSF intensity polarised by the amplitude filter for various

Values of (β=0,0.25,0.50,0.75,1), and it is clear from Figure 1 that the PSF intensity increases as the β values decrease. When β=0, the PSF peak=1 indicates that the light intensity distribution is greater in this region. It is noted from the curve that it is sharper, as this curve contains more than eighty four percent of the total intensity, and the rest is distributed in the secondary peaks, which is the Airy disk curve. As for the second curve for the intensity when β=0.25, it was shown that the intensity drops to less than 84% when entering the value (0.25), and we notice that the peak of the intensity drops to (0.70). When β=0.50 is entered, the central intensity drops more than the previous two curves, so that the peak intensity becomes 0.18. When β=0.75 is entered, the intensity decays, the peak PSF becomes (0.002), and the intensity distribution in the secondary peaks becomes higher than the previous curves. In Table 2, we have given the computed values of the quality evaluation whole width at half maximum, half width at half maximum for the amplitude filter, and diameter of the PSF; the term for the value at half of its maximum is referred to as the entire width at half maximum, where the whole width at half maximum the full width at half maximum (FWHM) is utilized to specify the breadth of any intensity distribution at half the maximum intensity in particular. The FWHM is used to determine the width of the beam, and the spectral width of light sources is often used, for example, when measuring the sharpness of spectral lines. The FWHM value describes how wide or narrow the spectral line is, describing the amount of light propagation. The data in Table 2 show that the FWHM value when β=0, 0.25, 0.50, and 1 is (2.63), indicating a good breadth of the energy distribution, while when β=0.75, the FWHM value is zero and indicates that the energy and light rays are not

International Journal of Applied Mathematics
Volume 38 No. 10s, 2025
ISSN: 1311-1728 (printed version); ISSN: 1314-8060 (on-line version)

distributed in this region. The Strehl ratio was calculated from Equation (9). Rayleigh showed that the intensity ratio is greater than or equal to 0.8 for the highly corrected system and that the intensity is greater than or equal to 0.7 for the system, including amounts of aberration. We showed the results in Figure 3. We notice that the Strehl criterion is at its best when β =0 and gradually decreases as the value of β increases.

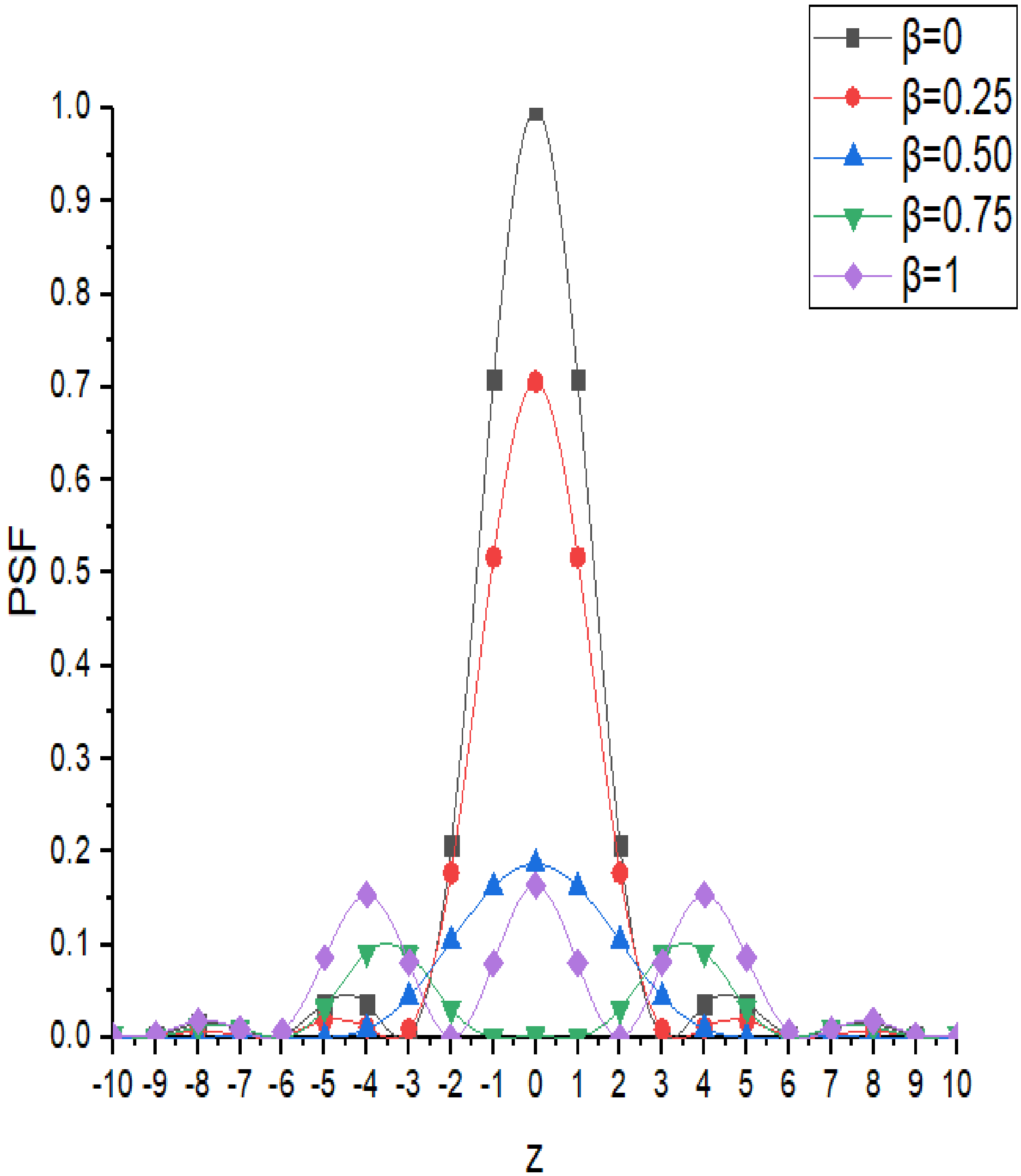

Figure 1: Shows the PSF intensity curves for a rectangular aperture when an amplitude hanning filter is applied to the optical system.

Received: August 03, 2025

International Journal of Applied Mathematics
Volume 38 No. 10s, 2025
ISSN: 1311-1728 (printed version); ISSN: 1314-8060 (on-line version)

z	β=0(PSF)	β=0.25(PSF)	β=0.50(PSF)	β=0.75(PSF)	β=1(PSF)
-10	0.00296	0.0009653	0.00041	0.003331	0.00235
-9	0.002097	0.001312	0.00009383	0.0006803	0.003208
-8	0.015	0.006823	0.0002243	0.012	0.018
-7	0.008809	0.002859	0.001366	0.011	0.008721
-6	0.002169	0.002082	0.00114	0.00004346	0.006531
-5	0.037	0.018	0.0001179	0.032	0.086
-4	0.036	0.011	0.009544	0.092	0.154
-3	0.002213	0.009451	0.044	0.09	0.081
-2	0.207	0.177	0.104	0.031	0.00005098
-1	0.708	0.517	0.162	0.0004638	0.08
0	1	0.706	0.187	0.002149	0.164
1	0.708	0.517	0.162	0.0004638	0.08
2	0.207	0.177	0.104	0.031	0.00005098
3	0.002213	0.009451	0.044	0.09	0.081
4	0.036	0.011	0.009544	0.092	0.154
5	0.037	0.018	0.0001179	0.032	0.086
6	0.002169	0.002082	0.00114	0.00004346	0.006531
7	0.008809	0.002859	0.001366	0.011	0.008721
8	0.015	0.006823	0.0002243	0.012	0.018
9	0.002097	0.001312	0.00009383	0.0006803	0.003208
10	0.00296	0.0009653	0.00041	0.003331	0.00235

Table 1: Shows the PSF intensity for different values of β for a rectangular aperture hanning amplitude filter.

β	PEAK (PSF)	FWHM	HWHM
0	1	2.63	1.31
0.25	0.70	2.63	1.31
0.50	0.18	2.63	1.31
0.75	0	0	0
1	0.16	2.63	1.31

Table 2: Measure the full width at half maximum and half width at half maximum of the apodized point spread function (PSF) for the specified values of β when a rectangular aperture.

International Journal of Applied Mathematics
Volume 38 No. 10s, 2025
ISSN: 1311-1728 (printed version); ISSN: 1314-8060 (on-line version)

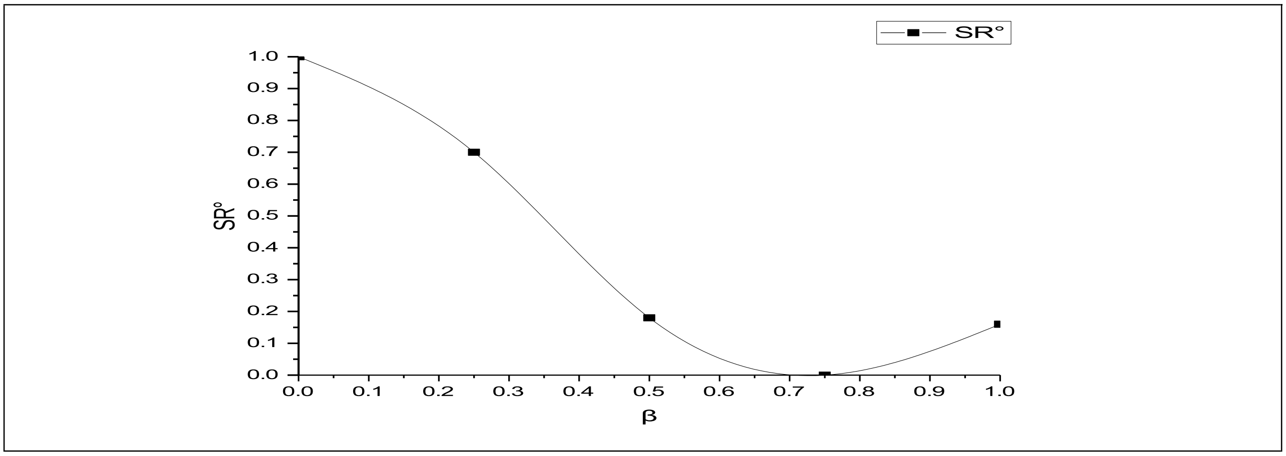

Figure 2:Variation of Strehl ratio (SR°) with β when a rectangular aperture.

A triangular aperture optical system was also used, where the PSF intensity of the triangular aperture was calculated using Equation No. 8, and the same Hanning amplitude filter was applied to it. The results were displayed graphically in Table No. 2 for the PSF values, where the results were displayed in Figure 3, showing the distribution of the PSF intensity polarised by the Hanning amplitude filter for various values of β: 0, 0.25, 0.50, 0.75, and 1. Figure 3 shows that when β = 1, 0, it gives the same intensity, which is the best value, which is 0.605. However, when β = 0.25 or 0.75, it also gives a similar intensity, which is 0.303, which gives the lowest intensity, and when β = 0.50, it gives a very low intensity, which is zero. When β =0.1, the intensity distribution of light is greatest in this region; when β =0.25 or 0.76, the intensity distribution is average. When β =0.50, the intensity distribution is poor. We presented the calculated values of the quality evaluation factor for the full width at half the maximum of the triangular aperture and half the width at half the maximum of the Hanning amplitude filter. The results are shown in Table 4, as this data facilitates our analysis. When β =0, 0.25, 0.75, and 1, the FWHM value is 1.99, indicating a good breadth of the energy distribution. When β =0.50, the full width at half the maximum value is zero, indicating that the energy and light rays are not distributed in this region. The Strel ratio for the triangular aperture was calculated from Equation 9. We presented the results in Figure 4. We note that the Strel criterion is at its best when β =0.1.

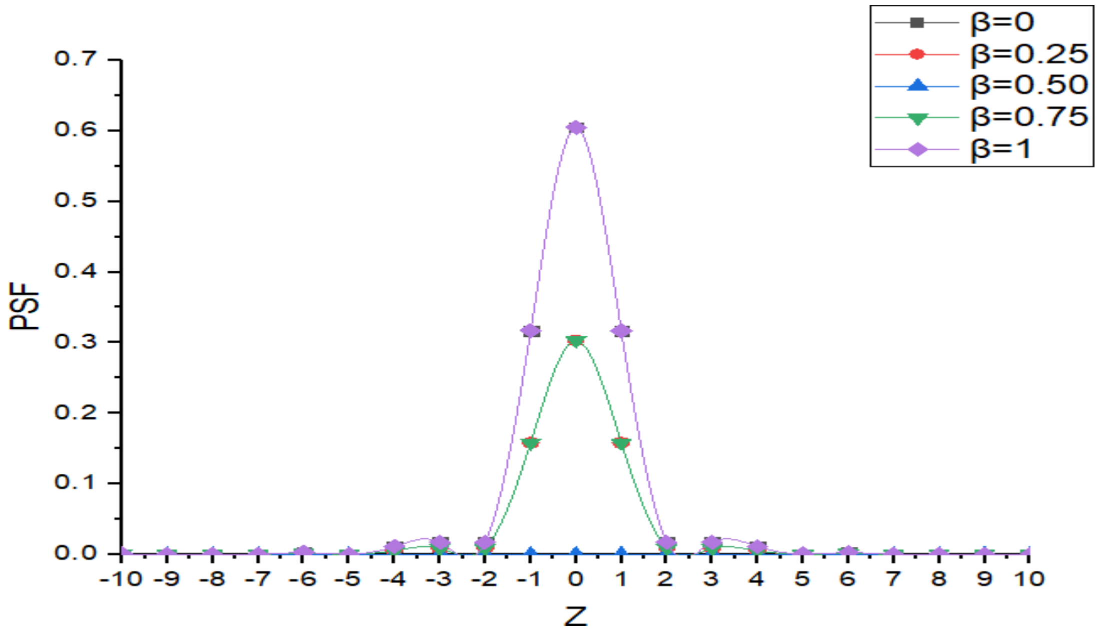

Figure 3: Shows the PSF intensity curves for a triangular aperture when an amplitude hanning filter is applied for the optical system.

z	β=0(PSF)	β=0.25(PSF)	β=0.50(PSF)	β=0.75(PSF)	β=1(PSF)
-10	0.000447	0.0002235	0	0.0002235	0.000447
-9	0.00009583	0.00004791	0	0.00004791	0.00009583
-8	0.000232	0.000116	0	0.000116	0.000232
-7	0.00001324	0.00000662	0	0.00000662	0.00001324
-6	0.002585	0.001293	0	0.001293	0.002585
-5	0.0004176	0.0002088	0	0.0002088	0.0004176
-4	0.011	0.005401	0	0.005401	0.011
-3	0.017	0.008555	0	0.008555	0.017
-2	0.017	0.008701	0	0.008701	0.017
-1	0.317	0.158	0	0.158	0.317
0	0.605	0.303	0	0.303	0.605
1	0.317	0.158	0	0.158	0.317
2	0.017	0.008701	0	0.008701	0.017
3	0.017	0.008555	0	0.008555	0.017
4	0.011	0.005401	0	0.005401	0.011
5	0.0004176	0.0002088	0	0.0002088	0.0004176
6	0.002585	0.001293	0	0.001293	0.002585
7	0.00001324	0.00000662	0	0.00000662	0.00001324
8	0.000232	0.000116	0	0.000116	0.000232
9	0.00009583	0.00004791	0	0.00004791	0.00009583
10	0.000447	0.0002235	0	0.0002235	0.000447

Table 3: Shows the PSF intensity for different values of β for a triangular aperture hanning amplitude filter.

Received: August 03, 2025

β	PEAK (PSF)	FWHM	HWHM
0	0.60	1.99	0.99
0.25	0.30	1.99	0.99
0.50	0	0	0
0.75	0.30	1.99	0.99
1	0.60	1.99	0.99

Table 4: Measure the full width at half maximum and half width at half maximum of the apodized point spread function (PSF) for the specified values of β when using a triangular aperture.

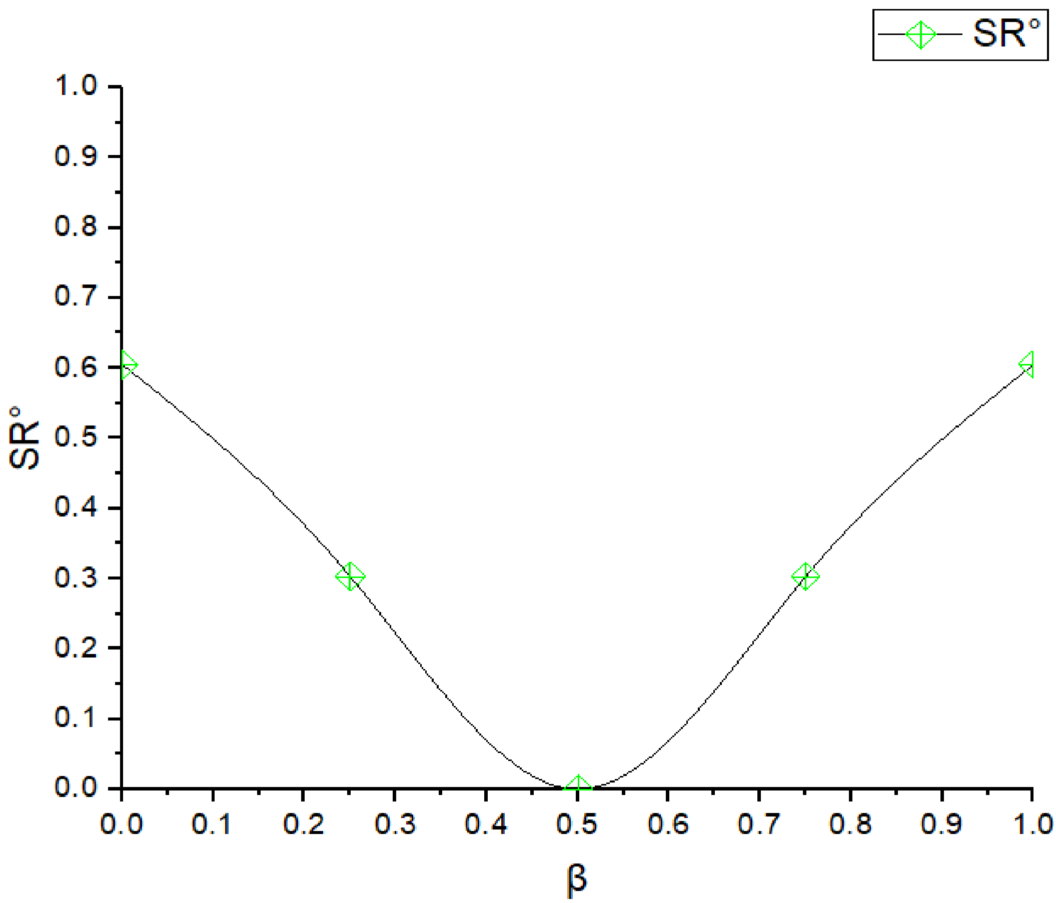

Figure 4: Variation of Strehl ratio (SR°) with β when a triangular aperture.

Conclusion:

In this study, the intensity redistribution of the polarized point distribution coefficient was determined for diverse values of B under the impact of a Hanning amplitude filter for a rectangular aperture optical system and a triangular aperture optical system. We analyzed the results utilizing half of the width maximum (FWHM). We note that when the FWHM is zero, this is not a realistic peak width for any actual measured peak. Between FWHM = 1.99 and FWHM = 2.36, 1.99 is the best choice if a sharper peak and higher resolution are desired, in which case the triangular aperture system is preferred. However, if more smoothing, better noise suppression, or a wider peak are desired for any reason, we choose FWHM = 2.63, in which case the rectangular aperture system is preferred.

Acknowledgement

The work was supported by Mustansiriyah University (www.uomustansiriyah.edu.iq), for which the authors are grateful.

References:

1. J. E. Sheedy and R. F. Hardy, "The optics of occupational progressive lenses," *Optom. Am. Optom. Assoc.*, vol. 76, no. 8, pp. 432–441, 2005.
2. C. E. Mungan, "Optical Images Due To Lenses And Mirrors," *J. Washingt. Acad. Sci.*, pp. 1–8, 2008.
3. Al-Shourbaji, I., Jabbari, A., Rizwan, S., Mehanawi, M., Mansur, P., & Abdalraheem, M. (2025). An Improved Ant Colony Optimization to Uncover Customer Characteristics for Churn Prediction. *Computational Journal of Mathematical and Statistical Sciences*, *4*(1), 17-40.
4. V, Sheela. (2025). ENHANCING ACADEMIC TRUST AND ACCOUNTABILITY: A SCALABLE BLOCKCHAIN SYSTEM FOR CREDENTIAL VERIFICATION FOR EDUCATION. International Journal of Applied Mathematics. 38. 803-819. 10.12732/ijam.v38i7s.516.
5. Nimma, D., Aarif, M., Pokhriyal, S., Murugan, R., Rao, V. S., & Bala, B. K. (2024, December). Artificial Intelligence Strategies for Optimizing Native Advertising with Deep Learning. In *2024 International Conference on Artificial Intelligence and Quantum Computation-Based Sensor Application (ICAIQSA)* (pp. 1-6). IEEE.
6. AlShourbaji, I., Helian, N., Sun, Y., & Alhameed, M. (2021). Customer churn prediction in telecom sector: A survey and way a head. *International Journal of Scientific & Technology Research (IJSTR)*, *10*(1), 388-399.
7. Sheela D V, and Chitra Ravi . “A Review on Secure Blockchain Integrated System for Technology Oriented Education Structure: Advantages and Issues.” International Research Journal on Advanced Science Hub 05.05S May (2023): 190–195. http://dx.doi.org/10. 47392/irjash.2023.S025
8. Dash, C., Ansari, M. S. A., Kaur, C., El-Ebiary, Y. A. B., Algani, Y. M. A., & Bala, B.

K. (2025, March). Cloud computing visualization for resources allocation in distribution systems. In *AIP Conference Proceedings* (Vol. 3137, No. 1). AIP Publishing.

9. Patel, Ahmed & Alshourbaji, Ibrahim & Al-Janabi, Samaher. (2014). Enhance Business Promotion for Enterprises with Mashup Technology. Middle East Journal of Scientific Research. 22. 291-299.
10. D. V. Sheela and R. Chitra, "Securing Online Quiz Management through Blockchain Technology and Three-Tier Cryptography with Hash-based Authentication," *2023 7th International Conference on I-SMAC (IoT in Social, Mobile, Analytics and Cloud) (I-SMAC),* Kirtipur, Nepal, 2023, pp. 135-144, doi: 10.1109/I-SMAC58438.2023.10290272.
11. Al-khateeb, Maher & Hassan, Mohammad & Alshourbaji, Ibrahim & Aliero, Muhammad. (2021). Intelligent Data Analysis approaches for Knowledge Discovery: Survey and challenges. İlköğretim Online. 20. 1782-1792. 10.17051/ilkonline.2021.05.196.
12. S. D. V and A. K. T. A, "Blockchain Integration for Enhanced Document Security and Access Control," *2025 6th International Conference on Data Intelligence and Cognitive Informatics (ICDICI),* Tirunelveli, India, 2025, pp. 609-614, doi: 10.1109/ICDICI66477.2025.11135382.
13. Elkady, G., Sayed, A., Priya, S., Nagarjuna, B., Haralayya, B., & Aarif, M. (2024). An Empirical Investigation into the Role of Industry 4.0 Tools in Realizing Sustainable Development Goals with Reference to Fast Moving Consumer Foods Industry. In *Advanced Technologies for Realizing Sustainable Development Goals: 5G, AI, Big Data, Blockchain, and Industry 4.0 Application* (pp. 193-203). Bentham Science Publishers.
14. Al-Shourbaji, I., Alhameed, M., Katrawi, A., Jeribi, F., Alim, S. (2022). A Comparative Study for Predicting Burned Areas of a Forest Fire Using Soft Computing Techniques. In: Kumar, A., Senatore, S., Gunjan, V.K. (eds) ICDSMLA 2020. Lecture Notes in Electrical Engineering, vol 783. Springer, Singapore. https://doi.org/10.1007/978-981-16-3690-5_22
15. Kaur, C., Al Ansari, M. S., Rana, N., Haralayya, B., Rajkumari, Y., & Gayathri, K. C. (2024). A Study Analyzing the Major Determinants of Implementing Internet of Things (IoT) Tools in Delivering Better Healthcare Services Using Regression Analysis. In *Advanced Technologies for Realizing Sustainable Development Goals: 5G, AI, Big Data, Blockchain, and Industry 4.0 Application* (pp. 270-282). Bentham Science Publishers.
16. A. N. K. Reddy, M. Hashemi, and S. N. Khonina, "Apodization of two-dimensional pupils with aberrations," *Pramana*, vol. 90, pp. 1–8, 2018.
17. F. S. Zainulabdeen, G. S. Karam, and Z. M. Abood, "Intensity Analysis for Optical System Apodized with Hanning Amplitude Filter," *Int. J. Mech. Eng.*, vol. 7, no. 1, pp. 1990–1996, 2022.
18. J. Lindberg, "Mathematical concepts of optical superresolution," *J. Opt.*, vol. 14, no. 8, p. 83001, 2012.

19. A. N. K. Reddy, R. Komala, M. K. Goud, and S. L. Goud, "A few PSF-based corollaries of optical systems apodized asymmetrically with two-dimensional complex pupil filters," *Arman. J. Phys.*, vol. 4, no. 4, pp. 200–205, 2011.
20. A. B. Hasan, "Efficiency Evaluation of Optical System Includes Different Stop Apertures When Using Relative Moving Factor," *NeuroQuantology.*, vol. 20, no. 4, pp. 211–215, 2022.
21. N. Q. Jouad, A. H. Al-Hamadani, R. A. Haleot, and G. S. Karam, "Image Resolution Enhancement for Parabolic Apodized Optical System," *Int. J. Mech. Eng.*, vol. 7, no. 1, pp. 1970–1977, 2022.
22. A. N. Kumar Reddy and D. K. Sagar, "Half-width at half-maximum, full-width at half-maximum analysis for resolution of asymmetrically apodized optical systems with slit apertures," *Pramana*, vol. 84, pp. 117–126, 2015.
23. A. H. Al-Hamadani, G. S. Karam, F. S. Zainulabdeen, Z. M. Abood, and A. Al-Saedi, "Study the effect of apodization on the imaging properties of optical systems with coma aberration," in *AIP Conference Proceedings*, 2019, vol. 2123, no. 1.
24. M. K. Devi, S. Ch, and T. V. Reddy, "Point Spread Function of Symmetrical Optical System Apodised with Gaussian Filte," *Int. J. Pure Appl. Physics. ISSN*, pp. 973–1776, 2018.
25. B. H. A. AlrueshdyM and A. F. H. Aldehadhawe, "Deriving And Calculation Of Point Spread Function For Array Of Obscured Circular Synthetic Apertures," *J. Univ. Babylon*, vol. 21, no. 5, pp. 1819–1827, 2013.
26. A. Narsaiah, T. K. Kumar, and D. K. Sagar, "Point Spread Functions Of Aberrated Optical Systems With Annular Apertures."
27. J. Campos, J. C. Escalera, A. Márquez, and M. J. Yzuel, "Pupil filters in optical systems. Implementation in liquid crystal spatial light modulators," *Asian J. Phys.*, vol. 23, no. 3, pp. 363–402, 2014.
28. M. Venkanna and D. K. Sagar, "PSF with Partial and Variable Apodization along with CPF," *Int. J. Eng. Technol. Manag. Appl. Sci.*, vol. 5, no. 6, 2017.
29. W. H. Tarkhan, "The Effect of Astigmatism Aberration on Point Spread Function for Optical System Using Different Apertures," *AL-Qadisiyah J. Pure Sci.*, vol. 23, no. 3, pp. 100–110, 2018.
30. Neil, Wilson, and Juskaitis, "A wavefront generator for complex pupil function synthesis and point spread function engineering," *J. Microsc.*, vol. 197, no. 3, pp. 219–223, 2000.
31. J. Luo, Y. Nie, W. Ren, X. Cao, and M.-H. Yang, "Correcting optical aberration via depth-aware point spread functions," *IEEE Trans. Pattern Anal. Mach. Intell.*, 2024.
32. A. H. Al-Hamadani, G. S. Karam, and A. S. Al-Saedi, "Apodization Defocused Optical Imaging System with Different Apertures using Hanning Amplitude Filter," *Adv. Phys. Theor. Appl.*, vol. 68, p. 5, 2017.
33. K. V. Kumar, B. Sambaiah, D. K. Sagar, and R. Sayanna, "Point spread functions of

defocused optical systems with hanning amplitude filters," *Int. J. Innov. Res. Sci. Eng. Technol*, vol. 2, pp. 4293–4297, 2013.
34. P. Thirupathi and T. R. Goud, "Strehl Ratio with Higher-Order Parabolic Filter"," *Int. OPEN ACCESS J. Mod. Eng. Res. ISSN*, pp. 2249–6645, 2014.
35. F. R. Kalaf and A. A. Raheem, "Improving the efficiency of thermal cameras using an optical filter," in *AIP Conference Proceedings*, 2025, vol. 3211, no. 1, p. 60018.
36. I. Chyzh, "Calculation of RMS Radiuses of the Point Spread Function Using Zernike Fringe Coefficients," in *Advanced System Development Technologies II*, Springer, 2025, pp. 41–65.
37. N. Qasim, G. S. Karam, A. H. Al-Hamadani, R. A. Haleot, and Z. M. Abood, "Calculation of ensquared energy of the diffraction-limited optical system with Higher-order parabolic filter," in *Journal of Physics: Conference Series*, 2021, vol. 1963, no. 1, p. 12078.
38. M. Zabic *et al.*, "Point spread function estimation with computed wavefronts for deconvolution of hyperspectral imaging data," *Sci. Rep.*, vol. 15, no. 1, p. 673, 2025.